



Properties and Application of 2000 MPa Grade Hot Stamping Steel

D. Zhang^(✉), J. L. Li, Y. Liu, Y. Li, Y. L. Qi, and P. Tao

Technology Center, Dongfeng Motor Group Co., Ltd., Wuhan 430058, China
zhangding@dfmc.com.cn

Abstract. In this paper, 2000 MPa hot stamping steel with Al-Si coating is studied in terms of material properties and process properties of steel plates, mechanical properties, process properties, ultimate sharp bending properties and hydrogen embrittlement susceptibility. And through the lightweight design and trial production case of the A-pillar and B-pillar reinforcement plates of a certain model under study, the lightweight effect and application feasibility of 2000 MPa hot stamping steel were analyzed. From the point of view of practical application, this steel has obvious technical advantages in lightening and replacing traditional HF1500 in safety parts of body structure without increasing the cost.

Keywords: 2000 MPa · Hot stamping steel · Lightweight

1 Introduction

Vehicle lightweighting has always been one of the important issues in the development of the world's automobiles, which plays an important role in the improvement of vehicle power economy and exhaust emission reduction. The development and application of ultra-high-strength steel is an important way to reduce the weight of automobiles and improve the safety. With the development of lightweight technology in automobiles and related industries, hot-formed steel sheets are widely used due to their advantages of high strength, good formability, and dimensional accuracy. Applied to body structural parts, the highest application ratio reaches 40% of the body-in-white weight.

Naderi [1] abroad studied a series of boron steels with different alloy compositions. The results show that 22MnB5, 27MnCrB5 and 37MnB4 can obtain a full martensitic structure through the hot forming process to achieve a strength level of 1500–2100 MPa. At present, PHS of 22MnB5 has been applied on a large scale, and PHS of 2000 MPa grade is also mass-produced by some steel mills. For example, ThyssenKrupp in Europe has developed 1900 MPa grade hot stamping steel MBW1900 based on 34MnB5 composition; Sweden SSAB Group has launched 2000 MPa grade hot stamping steel based on 37MnB4 composition. Stamping steel Docol2000Bor; Korean POSCO company developed 2000 MPa hot stamping steel HPF2000; ArcelorMittal company also developed 2000 MPa hot stamping steel USIBOR 2000, domestic such as Baosteel, Shougang, Angang, etc., Nippon Steel and Sumitomo Metal Group, China Iron and Steel Bao in

the Asia-Pacific region Wu Group Co., Ltd., etc., but only a few Japanese models and self-owned brand models have mass production applications.

Hot stamping refers to heating the steel plate to the austenitized state of 900–950 °C, using the high elongation of the steel plate in the austenitic state to carry out the stamping of complex parts and rapidly quenching in the mold to produce martensitic parts. Forming method, this process of forming first and then hardening perfectly solves the contradiction between strength and formability. Hot stamping steel with aluminum-silicon coating has always been a patented technology abroad. Hot stamping steel with 2000 MPa level is the first time in China that the development and application of steel grades are synchronized with foreign suppliers for application promotion. During the research and development process of a certain model of Dongfeng Motor Corporation, in order to reduce the weight and meet the five-star collision requirements of the 2021 version of C-NCAP, the characteristics and process performance of the material were studied.

2 Material Properties

2.1 Alloy Composition of Materials

The material of HF2000+AS150 developed by a steel company in China is selected. Its chemical composition is shown in Table 1. It can be seen that this steel is a C-Mn system. A small amount of Cr and Mo elements are added to improve the hardness of the substrate and refine the grains. Compared with the same series of HF1500, this steel grade significantly increases the content of C and Nb. Nb combines with C/N atoms in the steel to form a precipitation phase, which strengthens the matrix and provides hydrogen traps. The cost of alloying is more economical than HF2000 of other composition systems. According to the theoretical empirical formula [2], the CCT curve of HF2000 is calculated, as shown in Fig. 1, and the automatization temperature A_{c3} and martensitic transformation temperature M_s of the steel are calculated, as shown in Table 2. Compared with HF1500, the austenitizing temperature of HF2000 drops by about 30 °C, and the CCT curve shifts significantly to the right, which is compatible with the heat treatment process parameters of HF1500, and can also obtain full martensitic structure under air cooling. The hardness of the substrate reaches about 600 HV.

2.2 Material Properties After Heat Treatment

The flat die quenching of the test material was completed on the hot forming mass production line. In order to simulate the service performance of the actual vehicle, the

Table 1. Chemical composition.

Steel grade	Quality Score (wt.%)								
	C	Si	Mn	Cr	Mo	Alt	Ti	Nb	B
HF2000	0.38	0.25	1.16	0.19	0.199	0.038	0.042	0.051	0.0025
HF1500	0.25	0.30	1.21	0.183	/	0.041	0.035	0.005	0.0027

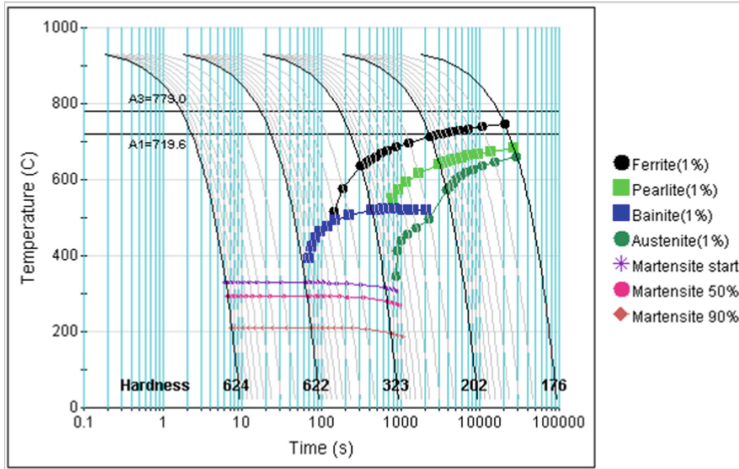


Fig. 1. CCT curve of theoretical calculation of steel grade.

Table 2. The theoretically calculated phase transition temperature of steel grades.

Steel grade	Ac3 (°C)	Ms (°C)
HF2000	779	329
HF1500	815	384

Table 3. Mass production process parameters of thermoforming production line.

Heating temperature/°C	Holding time/s	Transfer time/s	Holding pressure/t	Holding time/s
910–935	280	8	450	10

coating and baking process was simulated in an oven (170 °C, 20 min). The detailed parameters are shown in Table 3. Samples were taken from the steel plate along the rolling direction RD, and the uniaxial tensile properties and Vickers hardness were tested. From the test results in Table 4, the yield strength and elongation of the baked state are higher than those of the quenched state, the tensile strength is slightly reduced by about 150 MPa, and the hardness is unchanged, indicating that the baking does not change the C atoms in the martensite. The improvement of solid solution, strength and elongation benefits from the release of internal stress of quenched samples.

Combined with the specimens after quenched tensile fracture in Fig. 2(a), the fractures with specimen numbers 1#-1, 2#-3, 4#-3, 5#-3 and 6#-3 present it is flush and has no significant difference in tensile strength, indicating that the crack rapidly expands after reaching the maximum force and runs through the entire sample, and the local strain exceeds the material fracture limit at a low level, resulting in brittle fracture.

Table 4. Mechanical properties of materials after heat treatment.

Test Status	Specification mm	Tensile properties			Hardness
		Rp0.2/MPa	Pm/MPa	A50/%	HV1
Quenched state	1.5	1279	2078	5.1	556
	1.2	1311	2067	5.2	575
Baked state (170 °C/20 min)	1.5	1490	1973	7.5	556
	1.2	1477	1961	6.4	575

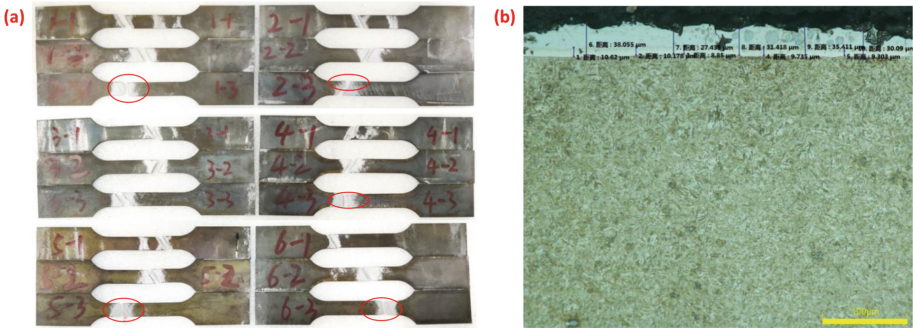


Fig. 2. Specimens after tensile and ultimate sharp bend tests: (a) Tensile specimen as quenched, (b) Microstructure and coating.

2.3 Ultimate Tip Bending Performance

The schematic diagram of the bending test is shown in Fig. 3, which is to characterize the ability of the body structure to bend and deform during the collision process. This method is widely used in the automotive industry to quickly measure the fracture strain of hot stamping steel. As shown in Fig. 3(b), during the bending process, the inner layer of the material is subjected to compressive stress, and the outer layer of the material is subjected to tensile stress. When the bending load reaches the peak, the outer surface of the material is affected by the tensile stress and begins to crack [3]. The test results in Table 5 show that the peak stress in the baked state has almost no change compared with the quenched state, but the maximum bending angle α_{max} has been significantly improved, indicating that the outer surface of the quenched state has a large residual tensile stress. After that, the tensile stress is released, and the local bending fracture limit is increased, which means that the application on crash safety parts can withstand higher bending deformation.

Compared with HF1500+AS150, which is currently widely used in body-in-white, the baked HF2000+AS150 fails to meet the requirement of 60° bending angle, but its maximum bending force is much larger than that of HF1500+AS150. Lightweight applications need to be combined with the design of specific body structures to evaluate their lightweight application effects (Fig. 4).

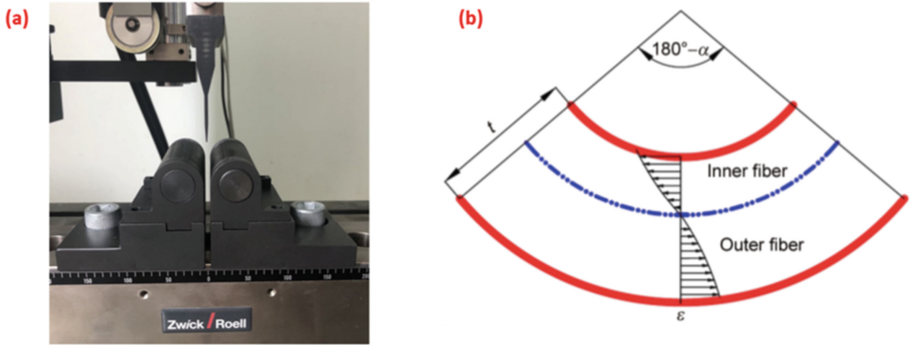


Fig. 3. Schematic diagram of VDA 238-100 bending and the distribution of strain in the thickness direction during the bending process.

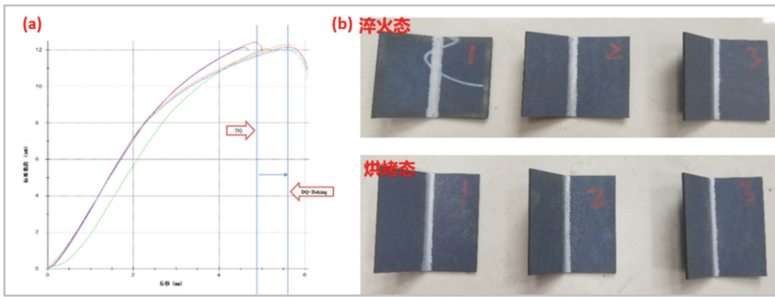


Fig. 4. Bending test of HF2000+AS150 test material.

Table 5. The extreme sharp cold bending angle of HF2000+AS150.

Specimen No.	Specimen state	Thickness t/mm	Maximum Force F/kN	Bending Angle α
1#	Quenched state	1.4	12.4	39°
2#		1.4	12.1	36°
3#		1.4	12.1	41°
4#	Baked state	1.4	12.3	51°
5#		1.4	12.2	52°
6#		1.4	12.0	54°
HF1500+AS150	Baked state	1.4	7.0	61°

2.4 Hydrogen Embrittlement Sensitivity Analysis of Materials

Hydrogen embrittlement delayed cracking is caused by the plastic damage caused by the hydrogen atoms in the steel. Some of the hydrogen atoms in the hot-formed steel come from the hydrogen in the steel, and part of it comes from the hydrogen flushing



Fig. 5. Hydrogen embrittlement susceptibility: (a) schematic diagram of TDS (Thermal Desorption Spectroscopy) test, (b) four-point bending specimen.

Table 6. Diffusible hydrogen content.

Dew point in furnace	Condition	Hydrogen content (ppm)
10 °C	Quenched state	0.18, 0.12, 0.20
10 °C	Baked state	0.04, 0.04, 0.04
<-15 °C	Quenched state	0.07, 0.11, 0.12
<-15 °C	Baked state	0.02, 0.02, 0.02

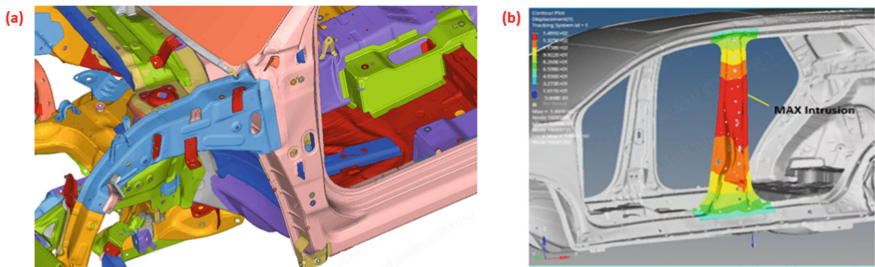
process in which the water vapor in the furnace is decomposed into H atoms during the hot stamping process. Literature [4] shows that when the local hydrogen concentration in the material exceeds 1.8 ppm, the material will undergo brittle cracking regardless of whether there is a stress field. When the concentration is lower than this, brittle cracking is the result of the combined action of hydrogen concentration and stress field.

First, select samples in different heat treatment states to measure the diffusible hydrogen content of the samples with TDS (Thermal Desorption Spectroscopy), and heating the samples at 400 °C can excite all the hydrogen atoms of the steel to overflow. The test results in Table 6 show that the hydrogen content of HF2000+AS150 is below 0.2 ppm, which is far less than the critical hydrogen concentration. Among them, the baking treatment has a significant effect on driving hydrogen, and the control of the dew point in the furnace also has an effect on reducing the hydrogen concentration in the steel. However, due to the aluminum-silicon coating on the surface of the material, the hydrogen atoms entering the furnace cannot easily escape, so the delayed cracking problem of the quenched HF2000+AS150 requires additional attention (Fig. 5).

Secondly, a constant load method is used to apply a certain stress to the baked material, which is supported by a special fixture and placed in a 0.1 mol/L HCl solution (pH = 1) for complete immersion. The immersed solution is updated every 24 h, and the target is soaked for 300 h, if any of the samples are broken, the test will be terminated early. Check whether the sample is broken every 12 h. The results in Table 7 show that when the constant load of HF2000+AS150 in a high-concentration hydrogen environment is less than or equal to 1200 MPa, the risk of delayed cracking can be basically controlled at a level comparable to that of HF1500+AS150. In fact, after coating and baking, the body components are covered with paint, and free hydrogen atoms from the external

Table 7. Hydrogen embrittlement susceptibility test.

Material	Loading stress	Fracture condition (total sample/fractured sample)		
		96 h	200 h	300 h
HF2000+AS150 Baked state	1.0 YS	5/1	-	-
	0.8 YS	5/0	5/0	5/0
HF1500+AS150 Baked state	1.0 YS	5/0	5/0	5/0

**Fig. 6.** C-NCAP collision simulation of 2021 version: (a) frontal collision, (b) side collision.

environment cannot enter the material. Therefore, it is necessary to design and control the stress of HF2000+AS150 during the application process.

3 Design of Lightweight Solutions

3.1 Collision Safety Performance

In order to meet the weight reduction and collision requirements of the model, the lightweight design and the safety design of the collision structure are carried out based on the scheme of the previous generation model. The thickness of the material is reduced. The simulation of frontal and side collisions was carried out according to the 2021 version of the C-NCAP test procedure using the digital model of the whole vehicle. The results in Fig. 6 show that the A-pillars (upper) and (lower) are almost not deformed under the frontal collision, maintaining the passenger compartment. The structure is stable, the intrusion of the B-pillar under the side collision at point P5 exceeds 125 mm, mainly because the large obstacle avoidance of the side-collision trolley pushes the entire B-pillar to move into the passenger compartment, and the body-in-white structure needs to be optimized. It is to meet the collision requirements of the 2021 version of C-NCAP.

3.2 Formability Simulation

For this lightweight solution, the formability simulation analysis was carried out. The results show that HF2000+AS150 can meet the forming requirements of the parts. The

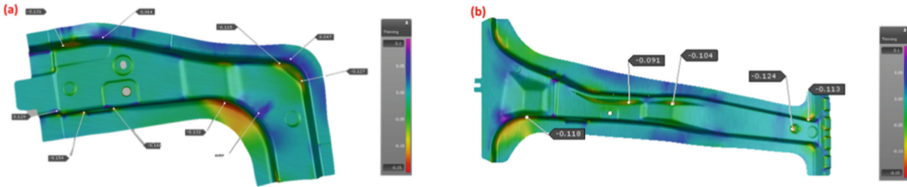


Fig. 7. Simulation analysis of hot stamping forming: (a) A pillar (bottom), (b) B pillar stiffener.

Table 8. Materials and weight reduction effects of lightweight solutions.

Previous-generation model		New model		Lightweight effect:	Cost change:
Materials	Crash Regulations	Materials	Crash Regulations	Part Weight Reduction	Total cost allocation
HF1500+AS150 1.4 mm & 1.8 mm & 2.0 mm	C-NCAP 2018	HF2000+AS150 1.2 mm & 1.5 mm	C-NCAP 2021	5 kg/Per Car	0

maximum thinning rate of the A-pillar (bottom) is 16.6%, which has the risk of stamping cracking. After local structural optimization, the thinning rate can be controlled within 15%, as shown in Fig. 7. The cost of parts is calculated by reducing the weight of a single vehicle by 5 kg. The increase in material grade does not bring about an increase in cost. The comparison of the plans is shown in Table 8.

4 Test Punch Verification of Parts and Vehicle Collision

On the mass production line of thermoforming, the most complex B-pillar reinforcement plate is used for trial punching, and the dew point of the production line is controlled between -15°C and -30°C . During the mold debugging stage, the delayed cracking of the hot-pressed parts occurred, as shown in Fig. 8. The cracking part is located at the R angle of the middle and lower transition zone of the B-pillar, and the crack originating position has obvious wear on the back door. After sampling and analysis of the same batch of failed samples and normal samples, the content of free hydrogen atoms and the tensile and VDA properties of the samples are comparable. The fracture at the origin of the crack is analyzed, the fracture is gray, and the microscopic morphology of the origin under the scanning electron microscope is an intergranular fracture, as shown in Fig. 8, which is judged to be a one-time brittle fracture.

The hardness of the tissue at the origin was tested, from the central part of the sample laterally and along the thickness direction from the surface interval $50\ \mu\text{m}$, the result is that the hardness of the surface close to the surface of the coating is the lowest 590 HV0.3, and the hardness from the surface to the core increases 40–50 HV0.3, while the core hardness range is 599–630 HV0.3. As discussed in the material development stage of Part 2 of this paper, the hardness of martensite depends on the content of C

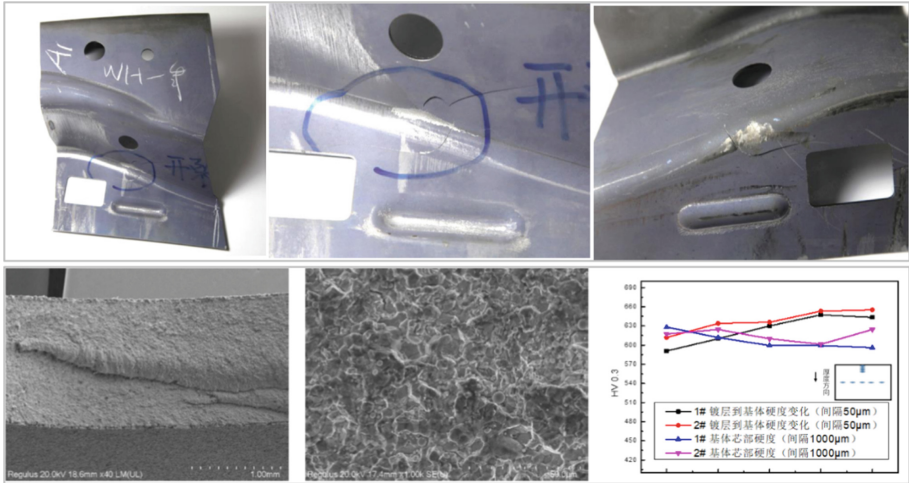


Fig. 8. Partial view of the delayed cracking part of the B-pillar, and fracture analysis and hardness testing at the origin of the crack.

element, and the C atoms in the austenite are concentrated in the martensite lattice due to the too fast cooling rate of the failed part., not only the phase transformation inside the part should be large, but also the martensite will produce twinning substructure due to too high C atoms, resulting in the material becoming brittle. At the same time, in the production process of the B-pillar reinforcement plate, the upper and lower molds were not fully ground at the R corner, resulting in local scratches, which became the origin of cracks.

Therefore, a new round of trial production was carried out by adjusting the gap between the upper and lower molds by grinding and closing the mold, and at the same time increasing the heating temperature of the heating furnace to 940–950 °C, reducing the heating time in the furnace from 320 s to 280 s. The hot-pressed parts were placed for 14 days without delayed cracking. The B-pillar was sampled and tested, as shown in Fig. 9. The hardness of the core sampled in different areas was 554–579 HV0.5, and the hardness distribution from the surface to the core showed an increase first and then decrease. Due to the mutual diffusion of Al-Si element in the coating and Fe-C in the matrix during the heating process, a gradient of C atomic enrichment is formed near the surface of the coating, and AlN precipitation is formed due to the Al element and the N element in the material. This results in an increase in local hardness, but the overall hardness distribution is relatively uniform. Sampling and testing the extreme sharp bending angle of the hot-pressed parts can reach 39–40°, and the maximum bending force is 11.9–12.3 KN, which has achieved the goal of the material development stage.

After the trial-manufactured and qualified parts are welded and loaded in the passenger car, the 2021 version of the C-NCAP crash test is carried out. The inspection of the sample is shown in Fig. 10. There is bending under the B-pillar reinforcement plate, which is disassembled from the inside of the vehicle. Observation in the cavity showed that the parts were intact and did not crack.

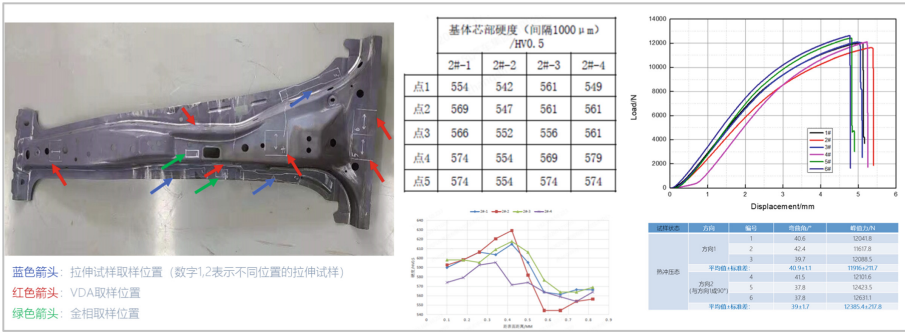


Fig. 9. Inspection and analysis of a new round of trial-produced samples.



Fig. 10. Sample inspection after side collision of 2021 version C-NCAP.

5 Conclusion

- (1) From the perspective of material properties, HF2000+AS150 has obvious lightweight benefits instead of HF1500+AS150, and the hot stamping process is compatible.
- (2) In the industrial production process of HF2000+AS150, there is a risk of hydrogen-induced delayed cracking. In addition to controlling the dew point in the furnace, the mold design should also be optimized to avoid uneven internal stress of phase transformation and twinned martensite.
- (3) From the perspective of local fracture toughness, although the extreme sharp bending angle of HF2000+AS150 does not reach the level of HF1500+AS150, due to its higher deformation resistance, the local strain during vehicle collision does not reach the fracture strain. Lightweight application on body structure safety parts is feasible.

References

1. M. Naderi, Hot stamping of ultra-high strength steels, Ph.d. thesis, Amirkabir University of Technology, (2007).
2. S. H. Zhang and C. J. Wu, *Iron and Steel Materials Science*, (Metallurgical Industry Press, 1992).
3. H. L. Yi, Z. Y. Chang, H. L. Cai, P. J. Du and D. P. Yang, Strength, plasticity and fracture strain of hot stamped steel, *Chinese Journal of Metals* **56**, 15 (2020).
4. J. X. Li, B. Kan and W. J. Wu, Stress-induced hydrogen diffusion and fracture behavior: A critical “true” hydrogen concentration for hydrogen-induced delayed cracking, in *Abstract collection of the 11th National Conference on Corrosion and Protection*, (Shenyang, China, 2021).

Open Access This chapter is licensed under the terms of the Creative Commons Attribution-NonCommercial 4.0 International License (<http://creativecommons.org/licenses/by-nc/4.0/>), which permits any noncommercial use, sharing, adaptation, distribution and reproduction in any medium or format, as long as you give appropriate credit to the original author(s) and the source, provide a link to the Creative Commons license and indicate if changes were made.

The images or other third party material in this chapter are included in the chapter’s Creative Commons license, unless indicated otherwise in a credit line to the material. If material is not included in the chapter’s Creative Commons license and your intended use is not permitted by statutory regulation or exceeds the permitted use, you will need to obtain permission directly from the copyright holder.

